Statistical properties of hurricane surge along a coast

Jennifer L. Irish,[1] Donald T. Resio,[2,3] and David Divoky[4]

Received 31 August 2010; revised 20 July 2011; accepted 25 July 2011; published 11 October 2011.

[1] The validity and accuracy of approaches used to determine hurricane surge hazard risk received much attention following the hurricane seasons in mid- to late-2000, which caused record surge-related damage along the Gulf of Mexico coastline. Following Hurricane Katrina in 2005, research showed that most extreme-value statistics approaches underestimated the risk associated with this surge event. In this paper, two of the most popular methods for determining hurricane surge extreme-value statistics are reviewed: the historical surge population approach and the joint probability method. Here, it is demonstrated that both limited historical record length and random along-coast variability in hurricane landfall location can introduce significant errors into surge estimates. For example, the historical surge population approach gives errors of 9% to 17% for return periods between 50 and 1000 years when a surge record of 100 years is considered. In contrast, it is shown that the joint probability method yields significantly more reliable surge estimates, with errors of 2% to 3% for return periods between 50 and 1000 years when a storm record of 100 years is considered. Finally, we show that both methods remain robust when decadal-scale climate variability in the storm rate of occurrence is considered, so long as the hurricane history is long enough to capture the full decadal cycle. When used in conjunction with continuous surge response information, it can be concluded that the joint probability method is a practical and reliable approach for determining extreme-value hurricane surge statistics.

Citation: Irish, J. L., D. T. Resio, and D. Divoky (2011), Statistical properties of hurricane surge along a coast, *J. Geophys. Res.*, *116*, C10007, doi:10.1029/2010JC006626.

1. Introduction

[2] An accurate and reliable estimation of coastal surge hazards is important for many reasons, including coastal planning, engineering design, evacuation planning, and communication of flood hazard to the public. The estimation of hurricane surge hazards has typically followed two very different approaches. In one approach, modeled surge values from historical storms are combined with information on historical storm frequencies to estimate local surge hazards; and in the other, modeled surge values from a set of parameterized storms are combined with information on the multivariate probabilities of the storm parameters to obtain similar estimates. To some extent, many scientists and engineers around the world have assumed that either approach, properly executed, will yield comparable estimates of actual hazard levels; hence, either of these would be acceptable for application to real-world problems. Given the critical need for accurate hazard estimates in coastal areas around the world, it is important to evaluate such an assumption in a very careful manner.

[3] In this paper, we review both commonly used methods, the historical surge population (HSP) approach and the joint probability method (JPM) in terms of the storm surge generated by a single storm and in terms of all surges generated by the general hurricane population. We show that, because of the relatively small spatial extent of high surges from individual storms combined with the small number of historical storms that produce large surges in a local sample, HSP approach introduces large errors in extreme-value estimates. In contrast, the JPM, which considers many more storms, albeit parameterized, yields statistically reliable surge estimates for comparable record lengths. Last, we investigate the potential role of climate variability, both secular and nonsecular decadal-scale variations, on hazard levels.

2. Background

2.1. The HSP and JPM Approaches

[4] In the HSP approach, surge values for the set of historical storms are obtained for some region of interest via a high-resolution surge model [e.g., *Bunya et al.*, 2010; *Dietrich et al.*, 2010] or from long-term water level gauge measurements. In the set of maximum values from each storm at a given location, the values are first ranked from lowest to highest. This infor-

[1]Department of Civil and Environmental Engineering, Virginia Polytechnic Institute and State University, Blacksburg, Virginia, USA.
[2]Coastal and Hydraulics Laboratory, U.S. Army Engineer Research and Development Center, Vicksburg, Mississippi, USA.
[3]Now at College of Computing, Engineering and Construction, University of North Florida, Jacksonville, Florida, USA.
[4]AECOM, Atlanta, Georgia, USA.

0148-0227/11/2010JC006626

mation is used to estimate a conditional cumulative distribution function (CDF) at this location from the relationship

$$F(\zeta_{\max}) = \frac{m}{N+1}, \tag{1}$$

where $F(\zeta_{\max})$ is the conditional CDF, i.e., probability of this surge, given that a storm occurred; m is rank of a surge with value $\zeta_{\max}$; and N is the total number of storms considered in the historical sample. If we assume that $F(\zeta_{\max})$ is time invariant, this can be related to return period $[T_R(\zeta_{\max})]$ by

$$T_R(\zeta_{\max}) = \frac{1}{\lambda[1 - F(\zeta_{\max})]}, \tag{2}$$

where λ is the rate of hurricane landfall occurrence, specified as the Poisson frequency parameter, taken to be the average number of hurricanes per year making landfall within some prescribed distance along the coast. Surge frequency is then determined by fitting a parametric (e.g., Gumbel, Weibull, generalized extreme-value (GEV)) or nonparametric (e.g., empirical simulation technique [*Borgman et al.*, 1992; *Scheffner et al.*, 1996]) distribution to the historical surge data.

[5] Introduced in the 1970s, the joint probability method (JPM) [e.g., *Ho and Myers*, 1975; *Myers*, 1975] considers the joint probability of a set of hurricane meteorological parameters at landfall, where the parameter set must be sufficient to define a parameterized wind field. In the 1970s such a parameterization would contain three explicit parameters: pressure deficit (defined as the peripheral pressure around the storm minus its central pressure), radius to maximum winds, and forward speed. In addition to these three parameters, two other parameters, related to the storm track, are critical to quantifying the storm surge at a fixed location. These are the angle of the track relative to the coast and the location of the point of interest relative to the hurricane's landfall point. *Holland* [1980] added an additional term, usually referred to as the "Holland B parameter," which influences the "peakedness" of the wind speeds within the storm. A limitation of the JPM in early applications was the assumption of constant parameter values all the way to the point of landfall during a hurricane's approach to the coast.

[6] Following Hurricane Katrina, the JPM and the HSP approach were revisited to assess both their accuracy for extreme-value statistics estimation and for their ability to quantify uncertainty in these statistical estimates [*Resio et al.*, 2009]. To overcome limitations in both the HSP approach and the traditional JPM, *Resio et al.* [2009] introduced a modified JPM that allows for (1) variability in meteorological conditions as storms approach the coast, (2) the development of continuous probability mass functions while using a reduced number of numerical storm simulations along with scaling laws [*Irish et al.*, 2009], and (3) a means for quantifying uncertainty. This JPM with optimal sampling (JPM-OS) is capable of providing a more statistically stable estimate of surge risk for rare events while using a manageable storm set for computational simulation.

[7] Since hurricane surge generation depends on both the meteorological characteristics of the hurricane and the response characteristics of the coast, the hurricane surge ($\zeta_{\max}$) for a given geographic location x may be written as

$$\zeta_{\max}(x) = \phi(x, x_o, c_p, R_p, \theta, v_f) + \varepsilon \tag{3a}$$

$$\varepsilon^2 = \varepsilon^2_{tide} + \varepsilon^2_{surge\ simulation} + \varepsilon^2_{waves} + \varepsilon^2_{winds} + \ldots \tag{3b}$$

where

ϕ a continuous surge response function;
x location of interest;
x_o landfall location;
c_p hurricane central pressure near landfall;
R_p hurricane pressure radius near landfall [*Thompson and Cardone*, 1996];
θ hurricane track angle with respect to the shoreline;
v_f hurricane forward speed near landfall;
ε uncertainty in the surge response [*Resio et al.*, 2009].

[8] Equation (3a) represents the expected surge generated, given known meteorological conditions (x_0, c_p, R_p, θ, v_f,) near landfall, while equation (3b) represents the uncertainty in the expected surge, for example, that is due to numerical surge simulation error and idealization of wind forcing.

[9] In the form of equations (3), the surge response is inherently dependent on probabilities associated with each hurricane meteorological parameter. By the JPM-OS approach [*Resio et al.*, 2009], a continuous probability density function (p) can be used to determine the return period:

$$T_R(\zeta_{\max}) = \left\{ 1 - \int_{c_p}\int_{R_p}\int_{v_f}\int_{\theta}\int_{x_o} p(c_p, R_p, v_f, \theta, x_o)[H(\zeta_{\max} - [\phi(x, c_p, R_p, v_f, \theta, x_o) + \varepsilon])]dx_o d\theta dv_f dR_p dc_p \right\}^{-1} \tag{4}$$

where H is the Heaviside step function, and by assuming the following form for p,

$$p(c_p, R_p, v_f, \theta, x_o) = \Lambda_1\Lambda_2\Lambda_3\Lambda_4\Lambda_5, \tag{5a}$$

$$\Lambda_1 = p(c_p|x_o) = \frac{1}{a_1(x_o)}\exp\left[-\frac{\Delta p - a_o(x_o)}{a_1(x_o)}\right] \cdot \exp\left\{-\exp\left[-\frac{\Delta p - a_o(x_o)}{a_1(x_o)}\right]\right\} \ (Gumbel\ Distribution) \tag{5b}$$

$$\Lambda_2 = p(R_p|c_p) = \frac{1}{\sigma(\Delta p)\sqrt{2\pi}} \cdot \exp\left\{-\frac{(\overline{R_p}(\Delta p) - R_p)^2}{2\sigma^2(\Delta p)}\right\} \ (Normal\ Distribution) \tag{5c}$$

$$\Lambda_3 = p(v_f|\theta) = \frac{1}{\sigma\sqrt{2\pi}} \cdot \exp\left\{-\frac{(\overline{v_f}(\theta) - v_f)^2}{2\sigma^2}\right\} \ (Normal\ Distribution) \tag{5d}$$

$$\Lambda_4 = p(\theta|x_o) = \frac{1}{\sigma(x_o)\sqrt{2\pi}} \cdot \exp\left\{ - \frac{\left(\overline{\theta}(x_o) - \theta\right)^2}{2\sigma^2(x_o)} \right\} \text{ (Normal Distribution)} \quad (5e)$$

$$\Lambda_5 = f(\lambda, x_o) \quad (5f)$$

where

Λ_I the probability density of an individual parameter;
Δp the central pressure deficit (peripheral pressure minus c_p);
a_i Gumbel coefficients;
σ normal distribution standard deviations;
overbars normal distribution mean values.

[10] In equations (5), the extreme-value distribution is assumed to be due to c_p only, whereas the distributions of R_p, θ, and v_f are assumed to normally distributed, with conditional dependence as indicated. The probability of hurricane landfall at a given location, Λ_5, is the rate of hurricane landfall occurrence per unit length of coast. The surge response function (ϕ) can be described in terms of scaling laws based on the governing physics for storm surge generation [*Irish et al.*, 2009], thus allowing the development of a continuous probability mass function via equations (5).

2.2. Inherent Uncertainties in the HSP Approach and the JPM

2.2.1. Statistical Uncertainty

[11] Several studies have now focused on the generalized pattern of surges along the coast generated by an individual hurricane [*Irish et al.*, 2009; *Irish and Resio*, 2010; *Resio et al.*, 2009]. It is clear that the distance from the landfall point to a fixed location of interest plays a dominant role in the surge that occurs at that point. As shown by *Irish et al.* [2009], the variation in surge levels along the coast scales with the storm size; and a shift in a storm's landfall location by a distance of only one to two times its radius to maximum winds, roughly 15 to 60 km, can produce a factor of 2 change in the peak surges at the fixed location of interest. Since the annual frequency of major hurricanes making landfall on the U.S. portion of the Gulf of Mexico, taken here as approximately 2000 km in the along-coast direction, is only about 0.36 hurricanes per year, we see that a fixed location might be expected to encounter relatively direct hits by only one to two major storms in 100 years. Of course, the actual hurricane frequency has been shown to vary markedly spatially within the Gulf of Mexico [*Interagency Performance Evaluation Task Force* (*IPET*), 2008], so this number is intended as only a very rough indicator of the number of storms in any specific area along the coast. Therefore, the number of samples of large surges in any localized area within the Gulf of Mexico will tend to be quite small. In turn, this suggests that the effects of random sampling will create very unstable estimates when based on only historical storms. Although the HSP approach often includes a large number of storms that make landfall at relatively large distances removed from a specific point of interest, the inclusion of these storms only very marginally influences the extreme surge probabilities, since these are almost entirely related to hurricanes that make landfall close to the point of interest. Also problematic when applying the HSP approach is that the storm sample often represents a limited set of meteorological conditions, namely, a limited number of central pressures, storm radii, track angles, and forward speeds.

[12] Variations in statistical characteristics of hurricanes have been found to vary on a much broader spatial scale than the scale of the alongshore variation in surge levels. For example, if we examine the variation in expected central pressures within the Gulf of Mexico given by *Levinson et al.* [2010] and approximate the pressure deficit term as 1012 mb – c_p, we can deduce that the pressure deficit term for a specified probability level, $p(c_p|x_0)$ varies by only about 20% along the entire U.S. Gulf of Mexico coast, about 2000 km. Additional studies [*IPET*, 2008] have shown that variations in storm frequency of about 50% occur over distances of about 400 km. On the other hand, the variation of surges along the coast is typically 50% or more within a distance equal to twice the radius to maximum winds, about 15 to 60 km: an order of magnitude smaller than the window for storm-frequency variation. *Chouinard et al.* [1997] provides a good statistical framework to estimate the scale of an appropriate sampling window for application to the definition of hurricane statistics. Using this method, it can be shown that, within the Gulf of Mexico, the optimal window size is about 580 km wide [*IPET*, 2008]. The appropriate scale for the along-coast variation in surges from individual event can be defined in terms of the average size in an "n-year" event; but this function will emerge naturally from the simulations conducted in this paper.

[13] In some executions of the HSP approach, the historical storm set for a fixed location is treated as the actual parent population and all aspects of uncertainty are examined only by "resampling" methods, such as the empirical simulation technique [*Scheffner et al.*, 1996]; however, this would be valid only if the historical record were essentially stationary and infinite in length. For hurricanes with their small spatial footprints of very high surges, it is obvious that the sampling variations can be very substantial. Thus, in surge studies it is important to recognize the existence of both types of uncertainty: the uncertainty in the historical sample and the uncertainty in what might happen over a given interval of time in the future. The JPM approach makes use of the slower variation in storm probabilities along a coast to extend the spatial sampling "window" considerably farther than the scale of the local surge response exhibited in the HSP approach. This is expected to allow the JPM to have much lower error bands for the first of these two types of uncertainty.

2.2.2. Model Uncertainty

[14] Measured surge levels usually do not yield sufficient spatial and temporal coverage to be useful on their own for extreme-value analysis. Thus, with the HSP approach and JPM alike, computational surge models are typically used to develop surge populations throughout a study region. These models introduce two types of uncertainty in the surge estimate. The first is the uncertainty that is due to limitations in model physics, for example, by bottom friction formulation, wind drag formulation, and numerical representation. The second is the uncertainty in model inputs, for example, because of errors in wind field representation and astronomical tide representation. This model uncertainty, e.g.,

equation (3b) for the JPM, is carried forward into the statistical analysis for both the HSP and JPM approaches. Also worth noting is that the measurements used to calibrate and verify surge models carry with them measurement uncertainty.

[15] Probably the most notable deficiency in the JPM approach is its dependence on parametric wind fields. Since it is not the error in the wind field but rather the impact of these errors on the surge heights that is relevant here, it is necessary to evaluate the potential impact of such parameterization numerically. For example, results from model simulations using the best-possible (nonparameterized) wind fields and results from model simulations using parameterized wind fields were compared with high water marks in Hurricanes Katrina and Rita (J. Westerink, University of Notre Dame, personal communication, 2010). This analysis suggests that the effect of using parameterized wind fields is to increase the random scatter in the comparisons without adding significantly to the bias. For our purposes, we shall assume, based on this numerical study, that the lack of specificity in the JPM wind fields leads to a 12% and 23% increase in the uncertainty variance, e.g., $\varepsilon^2_{\text{wind}}$ in equation (3b), of the final results, with no bias.

[16] In this paper, we investigate the HSP and JPM approaches in the context of minimizing statistical uncertainty.

3. Approach

[17] In this section, the capabilities of both the HSP and JPM approaches for estimating extreme-value statistics as a function of historical record length (K) and alongshore location of interest (x) are investigated, with the aim of answering the following question: How is the probability of large hurricane surges best characterized? Here we focus on the quantification of statistical uncertainty, and we do not consider model uncertainty. We further explore the sensitivity of both statistical approaches to time-varying meteorological conditions by considering time variation in hurricane rate of occurrence ($\lambda(t)$). For this purpose, we consider an idealized, uniform 2000 km long coastline subjected to parameterized hurricanes of constant forward speed v_f = 5.1 m/s and approach angle $\theta = 90°$ with respect to the coastline. In our paper we inherently assume that our sampling window for hurricane characteristics is 2000 km (i.e., the entire section of coast is homogeneous). If we consider that a 580 km width might be more appropriate for this, the net result would be to increase the uncertainty in the JPM estimates by a factor related to the effective decrease in the number of samples in the 580 km region from the number considered in the 2000 km region. Since essentially all estimates of uncertainty in extremal distributions depend on the square root of the number of samples, we can estimate this factor to be given by $\sqrt{2000/580} = 1.86$, such that the uncertainty when inhomogeneities in both the storm population and storm response are considered is 1.86 times the uncertainty when only an inhomogeneous response is considered.

3.1. Distribution for Sampling

[18] To develop synthetic storm histories, the hurricane probability distribution for sampling was assumed to be defined by the JPM probability mass function:

$$p(c_p, R_p, x_o) = \Lambda_1 \Lambda_2 \Lambda_5, \tag{6}$$

where the forms of Λ_1 and Λ_2 were specified by equations (5b) (Gumbel distribution) and (5c) (normal distribution). To simplify the analysis, the influence of forward speed and track angle were neglected. While these parameters indeed influence surge magnitude, *Irish et al.* [2008] showed that the relative influence of forward speed and track angle is small with respect to other factors. *Irish et al.* [2008] concluded that a 50% change in forward speed changes peak surge by no more than 20% and that changes in track angle change peak surge by no more than 10% with respect to a shore-normal approach, except for very oblique angles.

[19] The assumed actual distributions for c_p and R_p were taken to be representative of the U.S. Gulf of Mexico coastline. Based on analysis of hurricane observations at landfall on the U.S. Gulf of Mexico coastline, made by the National Oceanic and Atmospheric Administration [*Peterson and Baringer*, 2009], the c_p Gumbel coefficients are a_0 = 61 mbars and a_1 = 9 mbars, where the minimum (extreme) value for c_p was specified as c_p = 870 mbars [*Tonkin et al.*, 2000] using a maximum potential intensity (MPI) argument. The conditional relationship between R_p and c_p was assumed to have the following mean and standard deviation for a normal distribution:

$$\overline{R_p} = a(c_p - 900\text{mb}) + b, \tag{7a}$$

$$\sigma = c\overline{R_p}, \tag{7b}$$

where a, b, and c are constants, specified as a = 0.6 km/mbar, b = 26 km, and c = 0.4, based on R_p estimates developed by V. Cardone (Oceanweather Inc., personal communication, 2010) for the Gulf of Mexico historical record [*IPET*, 2008]. In equation (7), c_p is specified in millibars and R_p is specified in kilometers.

[20] The form of Λ_5 was taken to be uniform over the entire alongshore extent such that $\Lambda_5 = \lambda(t)/2000$ (per kilometer of coastline). The historical records of hurricane observations at landfall on the U.S. Gulf of Mexico coastline indicate a mean rate of occurrence of $\lambda(t) = \lambda = 0.36$ storms per year. For the case of time-invariant meteorological conditions, λ is assumed constant in time and applied uniformly over the 2000 km coastline length. This same historical record exhibits decadal-scale variations in rate of occurrence, with roughly 10 years of high activity followed by roughly 30 years of low activity. For the case of time-varying meteorological conditions, $\lambda(t)$ is specified as 1.14 for 10 years, then as 0.10 for 30 years; $\lambda(t)$ is applied uniformly over the 2000 km coastline.

[21] The surge response function was specified using the scaling laws of *Irish et al.* [2009],where the dimensionless surge response function (SRF) is defined in terms of the dimensionless surge ($\xi'_{\max}(x)$),

$$\zeta'_{\max}(x) = \frac{\gamma \zeta_{\max}(x)}{\Delta p} + m(x)\Delta p, \tag{8a}$$

and the dimensionless alongshore distance from location of interest to peak surge (x'):

$$x' = \frac{(x - x_o)}{R_p} - \delta \tag{8b}$$

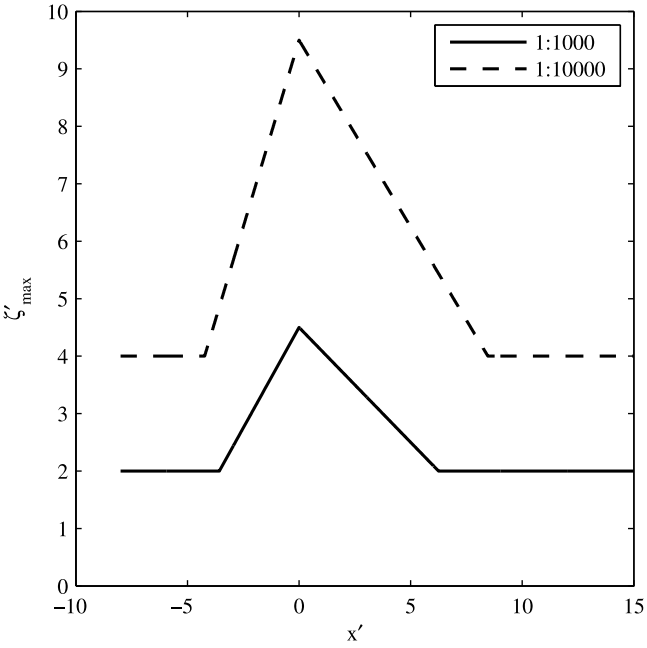

Figure 1. Dimensionless surge response functions for any location (x) along an idealized coastline fronted by a 1:1000 or 1:10,000 continental shelf slope.

where γ is the specific weight of water, $m(x)$ is a location-dependent constant, and δ is the average distance between landfall location (x_0) and peak alongshore surge normalized by R_p.

[22] For an idealized coast representing the northern Gulf of Mexico shoreline, two SRFs were approximated as triangular SRF distributions (Figure 1) based on idealized numerical hurricane surge simulations [*Irish et al.*, 2008] to represent the surge response at the coast for hurricanes propagating over two geometries: (1) a mildly sloping continental shelf (1:10,000) and (2) a moderately sloping continental shelf (1:1000). Because alongshore uniformity is assumed in this analysis, the SRF does not change with location along the coastline. Furthermore, we assume that the SRF is a perfect solution for ζ_{max} in equation (3a), such that the surge response uncertainty term ε^2 is zero. The surge-frequency relationships, using these idealized SRFs and the sample distribution in equation (6), by the JPM, are given in Figure 2. While idealized geometries are considered here, SRFs have been shown to perform well for real coasts, with root-mean-square (RMS) errors of less than 0.25 m (less than 9%) with respect to computational simulation [*Irish et al.*, 2009].

[23] Using the above described actual distribution, synthetic storm histories were developed for historical record lengths of K = 25, 50, 100, 200, 500, 1000, 10,000, and 100,000 years. The number of storms per year within the history was based on random-number sampling over the interval from 0 to 1 of the Poisson distribution described by $\lambda(t)$. For each storm within the synthetic record, the landfall location was determined by random-number sampling over the 2000 km coastline length. For the case of time-varying rates of occurrence, the starting point within the 40 year cycle was determined by random-number sampling. Finally, c_p and R_p for each storm were similarly determined by random-number sampling over their respective CDF intervals, from 0 to 1. In all, synthetic storm histories were developed for each record length until convergence was achieved; up to 1200 histories per record length were generated. For each synthetic storm history, surge CDFs were computed at 10 km intervals along the idealized coastline using the JPM and using the HSP approach.

3.2. Application of the JPM

[24] In applying the JPM to each synthetic record, the JPM probability mass function was determined for each synthetic record; then the surge CDF was developed using the SRFs shown in Figure 1. For the purposes of this study, which focuses on extreme value statistics of surge, the JPM probability mass function was specified using equation (6), as follows:

[25] 1. As with the distribution for sampling, the influence of forward speed and track angle was not considered.

[26] 2. The probability of hurricane landfall was assumed to be uniform throughout the idealized coast and was specified as $\Lambda_5 = \lambda(t)/2000$ (per kilometer of coastline).

[27] 3. The central pressure probability Λ_1 was assumed to follow a Gumbel distribution, equation (5b). For each record, the Gumbel coefficients a_0 and a_1 were determined, where the minimum (extreme) value for c_p was specified as c_p = 870 mbars [*Tonkin et al.*, 2000] using a maximum potential intensity (MPI) argument.

[28] 4. The hurricane pressure radius probability Λ_2 was assumed to follow a normal distribution, equation (5b), with mean and standard deviation dependent on central pressure, equation (7). For each record, the coefficients a, b, and c in equation (7) were determined in order to specify the mean and standard deviation of the normal distribution.

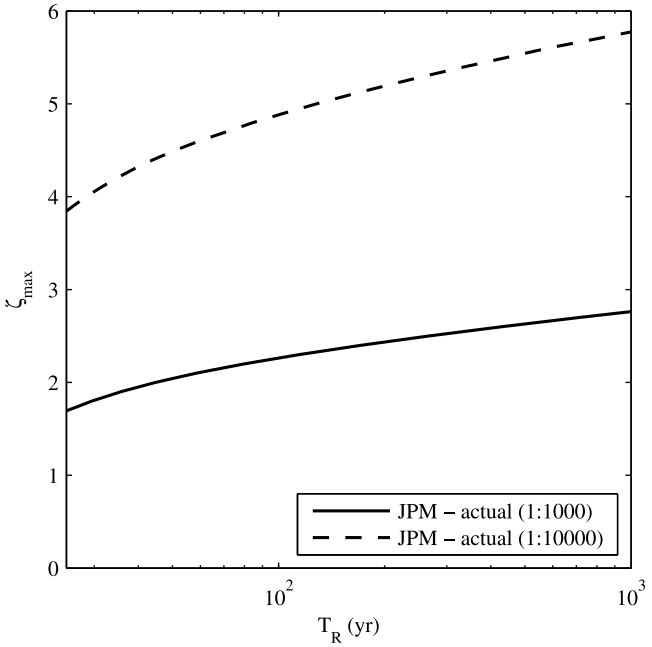

Figure 2. Actual surge stage frequency relationships based on assumed actual meteorological parameter distribution and idealized numerical surge simulations.

3.3. Application of the HSP Approach

[29] A peaks-over-threshold (POT) method was employed to develop surge CDFs using the HSP approach, as follows:

[30] 1. The POT threshold was taken as $\zeta_{max} \geq 0.86$ m for the 1:1000 slope case and $\zeta_{max} \geq 1.88$ m for the 1:10,000 slope case; POT thresholds were selected so that convergence of the HSP estimates occurred when record length $K \geq 10{,}000$ yr.

[31] 2. A parametric generalized extreme-value (GEV) distribution was assumed when the number of surge events in the POT population was greater than or equal to 5; if the number of surge events was less than 5 but greater than 3, a Gumbel distribution was assumed.

[32] 3. A quality check was imposed on the resulting GEV distributions: When the resulting GEV distribution resulted in a 1000 year return period surge larger than $\zeta_{max} \geq 6.00$ m for the 1:1000 slope case and $\zeta_{max} \geq 12.00$ m for the 1:10,000 slope case, the distribution was recomputed by assuming a Gumbel distribution. These evaluation surges of 6.00 and 12.00 m represent surge values that are 75% higher than the largest surges appearing in the synthetic records.

[33] 4. When the POT population contained fewer than three surge events, a no-value result was recorded.

3.4. Error Statistics

[34] To assess the capabilities of both the HSP approach and the JPM, two types of error statistics were evaluated: root-mean-square (RMS) error and mean error. Additionally, the individual record error was assessed. For JPM error statistics, the JPM-computed extreme-value surges for each record length (ζ_{JPM-K}) were compared against the extreme-value surges computed with the JPM when the probability distribution for sampling was used ($\zeta_{JPM\text{-}actual}$). For HSP error statistics, the HSP-computed extreme-value surges for each record length (ζ_{HSP-K}) were compared against the mean result for extreme-value surges computed with the HSP approach when $K = 100{,}000$ yr ($\bar{\zeta}_{HSP-100000}$). The error for each realization, $\Delta\zeta_{max}(n)$, was computed as follows:

$$\Delta\zeta_{max}(n)_{JPM} = \zeta_{JPM-K}(n) - \zeta_{JPM-actual}, \tag{9a}$$

$$\Delta\zeta_{max}(n)_{HSP} = \zeta_{HSP-K}(n) - \bar{\zeta}_{HSP-100000}, \tag{9b}$$

where n is the record number. The RMS error was computed as follows:

$$JPM\ RMS\ error = \sqrt{\frac{\sum_1^n \Delta\zeta_{max}(n)^2_{JPM}}{N}}, \tag{10a}$$

$$HSP\ RMS\ error = \sqrt{\frac{\sum_1^n \Delta\zeta_{max}(n)^2_{HSP}}{N}}, \tag{10b}$$

where N is the total number of records. Similarly, the mean error was computed as follows:

$$JPM\ mean\ error = \frac{\sum_1^n \Delta\zeta_{max}(n)_{JPM}}{N} \tag{11a}$$

$$HSP\ mean\ error = \frac{\sum_1^n \Delta\zeta_{max}(n)_{HSP}}{N} \tag{11b}$$

The RMS and mean errors were computed for each record length at return periods of $T_r = 50$, 100, 500, and 1000 years.

4. Results

4.1. Impact of Historical Record Length

[35] The influence of record length (K) and mean storm frequency ($\lambda(t) = \lambda$) on extreme-value statistics was quantified by evaluating RMS and mean errors in the probability predictions based on both the JPM and the HSP approach, with respect to the assumed actual distribution, at return periods of $T_R = 50$–1000 years. For this evaluation, the HSP results for the midpoint along the coast ($x = 1000$ km) are considered. The RMS error and mean error in surge predictions for synthetic record lengths from $K = 25$–to 10,000 years, for both the HSP approach and the JPM, are given in Tables 1 and 2. For all record lengths, the RMS errors in the JPM estimate are no more than 0.15 m (7%) and 0.27 m (6%) with respect to the actual assumed surge distribution for the 1:1000 and 1:10,000 continental shelf slope cases, respectively. Mean errors with the JPM are very small; for most record lengths and return periods, the mean error is within ±0.02 m (±1%).

[36] The results reveal two shortcomings of the HSP approach. First, the number of surge events over the specified threshold is often too low to yield meaningful statistics. This is particularly true when the record length is less than $K = 50$ years. For the 1:1000 slope case, 17% of the $K = 50$ years synthetic records contained fewer than three surge events, such that a no-value result was recorded. For the 1:1000 slope case, 65% of the $K = 25$ years synthetic records yielded a no-value result. Because of the more widespread, higher surges associated with hurricane propagation over milder slopes, the number of no-value results for the 1:10,000 slope case is somewhat less than that of the 1:1000 case: 53% and 10% for the $K = 25$ and 50 year record lengths, respectively.

[37] Second, and as expected, the results show that record length has a large impact on the accuracy of surge predictions when using the HSP approach. Here, the RMS and mean errors in extreme-value statistics in Tables 1 and 2 reflect only the errors associated with records with more than three surge events. On average, the percentage of RMS errors in the surge level when the record length $K = 25$ years is 27% and 17% for the 1:1000 and 1:10,000 continental shelf slope cases, respectively; the HSP surge estimations yield RMS errors of at least 0.26 m and 0.56 m. As record length increases, the RMS error in the HSP surge estimates over the entire range of T_R decreases. For the 1:1000 slope case, the RMS error in the HSP estimate is reduced to that of the $K = 25$ year JPM estimate (7%) for record lengths longer than $K = 200$ years. For the 1:10,000 slope case, the reduction in the RMS error in the HSP estimate to that of the $K = 25$ year JPM estimate (6%) is not achieved until the record length is longer than $K = 500$ years.

[38] HSP convergence values for both the 1:1000 and 1:10,000 slope cases show a bias with respect to the assumed actual distribution. At convergence, the HSP values for both slope cases exhibit negative biases (−3% to −5%) for smaller return periods and exhibit positive biases (+1% to +4%) for return periods of $T_R \geq 500$ years. The observed biases in the HSP approach are likely due to the

Table 1. Root-Mean-Square and Mean Error in Surge Estimates as a Function of Statistical Approach and Record Length for an Idealized Coastline Fronted by a 1:1000 Continental Shelf Slope[a]

	JPM RMS Error (m) [Mean Error (m)]					
K (years)	T_R = 50 Years, Surge = 2.04 m	T_R = 100 Years, Surge = 2.26 m	T_R = 500 Years, Surge = 2.63 m	T_R = 1000 Years, Surge = 2.76 m	Percent With No Result	Average RMS Error (m)
25	0.15 [−0.05]	0.12 [−0.01]	0.14 [0.02]	0.15 [0.02]	0	0.14
50	0.09 [−0.03]	0.08 [−0.01]	0.09 [0.00]	0.11 [0.01]	0	0.09
100	0.06 [0.00]	0.05 [0.00]	0.07 [0.01]	0.07 [0.01]	0	0.06
200	0.04 [0.00]	0.04 [0.00]	0.05 [0.01]	0.05 [0.01]	0	0.04
500	0.03 [0.01]	0.02 [0.01]	0.03 [0.01]	0.03 [0.01]	0	0.03
1,000	0.02 [0.01]	0.02 [0.01]	0.02 [0.01]	0.02 [0.01]	0	0.02
10,000	0.01 [0.01]	0.01 [0.01]	0.01 [0.01]	0.01 [0.01]	0	0.01
100,000	0.02 [0.02]	0.01 [0.01]	0.01 [0.01]	0.01 [0.01]	0	0.01
	HSP RMS Error (m) [Mean Error (m)] at x = 1000 m					
K (years)	T_R = 50 Years, Surge = 1.98 m	T_R = 100 Years, Surge = 2.24 m	T_R = 500 Years, Surge = 2.70 m	T_R = 1000 Years, Surge = 2.87 m	Percent With No Result	Average RMS Error (m)
25	0.26 [0.06]	0.29 [−0.09]	0.49[−0.40]	0.58 [−0.52]	65	0.41
50	0.23 [0.00]	0.26 [−0.12]	0.47 [−0.39]	0.57 [−0.49]	17	0.38
100	0.20 [−0.01]	0.22 [−0.09]	0.39 [−0.28]	0.48 [−0.35]	0	0.32
200	0.14 [−0.01]	0.14 [−0.05]	0.27 [−0.16]	0.36 [−0.20]	0	0.23
500	0.10 [0.00]	0.10 [−0.02]	0.16 [−0.07]	0.21 [−0.09]	0	0.14
1,000	0.06 [0.00]	0.06 [−0.01]	0.12 [−0.02]	0.16 [−0.02]	0	0.10
10,000	0.02 [0.00]	0.02 [0.00]	0.03 [0.00]	0.04 [−0.01]	0	0.03
100,000	0.01 [0.00]	0.01 [0.00]	0.01 [0.00]	0.01 [0.00]	0	0.01

[a]RMS, root-mean-square. Average RMS error represents average for all T_R between 50 and 1000 years.

assumed parametric fit, in which the parametric CDF tends to be more steeply sloping than that of the assumed actual distribution. These biases largely describe the computed RMS errors associated with the HSP approach at convergence.

4.2. Impact of Alongshore Position

[39] For any given historical hurricane history, the set of landfall positions relative to the location of interest varies from point to point along the coast. This effect results in different surge data populations for each alongshore location x. For example, one K = 50 year synthetic history is given in Table 3, showing surge values at five locations along the coast. In this sample history, the highest surge value differs by more than 1 m, where the highest surge at x = 900 km is 37% lower than the highest surge at x = 1500 km. In fact, the highest surge at x = 900 km in this history is 18% lower than the highest surge just 100 km to the east at x = 1000 km. For such short histories it is then

Table 2. Root-Mean-Square and Mean Error in Surge Estimates as a Function of Statistical Approach and Record Length for an Idealized Coastline Fronted by a 1:10000 Continental Shelf Slope[a]

	JPM RMS Error (m) [Mean Error (m)]					
K (years)	T_R = 50 Years, Surge = 4.49 m	T_R = 100 Years, Surge = 4.88 m	T_R = 500 Years, Surge = 5.54 m	T_R = 1000 Years, Surge = 5.77 m	Percent With No Result	Average RMS Error (m)
25	0.27 [−0.09]	0.21[−0.02]	0.24 [0.03]	0.27 [0.04]	0	0.24
50	0.17 [−0.05]	0.14 [−0.02]	0.17 [0.01]	0.19 [0.01]	0	0.16
100	0.11 [0.00]	0.10 [0.01]	0.12 [0.02]	0.13 [0.02]	0	0.11
200	0.08 [0.00]	0.07 [0.00]	0.08 [0.01]	0.09 [0.01]	0	0.08
500	0.05 [0.02]	0.04 [0.02]	0.05 [0.02]	0.06 [0.02]	0	0.05
1,000	0.03 [0.02]	0.03 [0.02]	0.04 [0.02]	0.04 [0.02]	0	0.04
10,000	0.03 [0.02]	0.02 [0.02]	0.02 [0.02]	0.02 [0.02]	0	0.02
100,000	0.03 [0.03]	0.02 [0.02]	0.02 [0.02]	0.02 [0.02]	0	0.02
	HSP RMS Error (m) [Mean Error (m)] at x = 1000 m					
K (years)	T_R = 50 Years, Surge = 4.25 m	T_R = 100 Years, Surge = 4.73 m	T_R = 500 Years, Surge = 5.62 m	T_R = 1000 Years, Surge = 5.93 m	Percent With No Result	Average RMS Error (m)
25	0.52 [−0.01]	0.62 [−0.30]	1.04 [−0.89]	1.23 [−1.10]	53	0.86
50	0.45 [−0.04]	0.52 [−0.28]	0.92 [−0.79]	1.11 [−0.97]	10	0.76
100	0.37 [−0.03]	0.41 [−0.18]	0.74 [−0.53]	0.92 [−0.65]	1	0.61
200	0.26 [−0.04]	0.28 [−0.10]	0.54 [−0.23]	0.70 [−0.27]	0	0.44
500	0.17 [−0.01]	0.18 [−0.03]	0.32 [−0.09]	0.44 [−0.10]	0	0.27
1,000	0.11 [0.00]	0.11 [−0.01]	0.22 [−0.04]	0.30 [−0.05]	0	0.18
10,000	0.04 [0.00]	0.04 [−0.01]	0.06 [−0.01]	0.08 [−0.01]	0	0.05
100,000	0.01 [0.00]	0.01 [0.00]	0.02 [0.00]	0.03 [0.00]	0	0.02

[a]RMS, root-mean-square. Average RMS error represents average for all T_R between 50 and 1000 years.

Table 3. Sample Synthetic Surge Histories at Varying Alongshore Locations for a Record Length of K = 50 Years for the Case of a 1:1000 Continental Shelf Slope[a]

c_p (mb)	R_p (km)	x_o (km)	x = 500 km	x = 900 km	x = 1000 km	x = 1100 km	x = 1500 km
911	32	1,435	<thres	<thres	<thres	<thres	**3.06**
934	47	96	<thres	<thres	<thres	<thres	<thres
936	41	709	<thres	1.73	0.96	<thres	<thres
941	49	1,010	<thres	<thres	1.89	**2.49**	<thres
943	83	1,155	<thres	<thres	1.02	1.62	1.78
945	47	340	1.95	<thres	<thres	<thres	<thres
945	68	452	**2.26**	1.07	<thres	<thres	<thres
946	85	232	2.00	<thres	<thres	<thres	<thres
947	36	1,022	<thres	<thres	1.59	2.24	<thres
949	59	1,369	<thres	<thres	<thres	<thres	2.18
949	43	933	<thres	1.48	**2.35**	1.74	<thres
951	75	473	1.95	1.25	0.91	<thres	<thres
953	27	290	<thres	<thres	<thres	<thres	<thres
953	49	765	<thres	**1.94**	1.44	0.94	<thres
955	81	330	2.05	0.88	<thres	<thres	<thres
955	27	1,289	<thres	<thres	<thres	<thres	<thres
956	66	1,792	<thres	<thres	<thres	<thres	<thres
959	68	1,899	<thres	<thres	<thres	<thres	<thres

[a]Highest surge event at each location is in bold, and "<thres" indicates surge was less than threshold value for peaks-over-threshold method.

expected that, in using the HSP approach, surge estimates along the coast will artificially vary in direct consequence of the landfall locations represented in the history.

[40] Figures 3 and 4 show the alongshore variations in the surge estimates for T_R = 100 and 500 years for a representative set of synthetic histories. Because the JPM considers all possible tracks regardless of those included in the historical record, no alongshore variation in the surge estimates is present. These figures, however, do show that the HSP approach yields different surge estimates at different locations along the coast. This finding is consistent with that of *Agbley and Basco* [2008]. Additionally, this analysis shows that with increasing record length, this alongshore variation diminishes in magnitude and becomes more slowly varying alongshore.

[41] Table 4 presents the variability in the extreme-value statistics. In the table, the alongshore-wise standard deviations in surge estimates are presented. This table shows that for short record lengths of K = 50 years, the surge estimate varies between 12% and 16% from location to location, with respect to the average alongshore surge estimate obtained by the HSP approach. The results further demonstrate that as record length increases, the alongshore variation in the surge estimate diminishes, indicating a convergence with increased record length. This is a direct consequence of better representation of landfall location possibilities within the historical population. Convergence, to about 1%, from location to location alongshore is achieved with very long record lengths of K = 10,000 yr.

4.3. Impact of Decadal-Scale Variations in Hurricane Rates of Occurrence

[42] The analysis presented in section 4.1 was repeated for the case in which the rate of occurrence varied in time: $\lambda(t)$ is specified as 1.14 for10 years and then as 0.10 for 30 thirty years. Results using the JPM for record lengths K = 50–10,000 years show no measurable difference between the extreme-value estimates when λ is constant and when it is variable. Over the range of T_R = 50–1000 years, the RMS errors computed when varying $\lambda(t)$ are assumed to differ by no more than 1% from the RMS errors computed when a constant value of λ is assumed (e.g., those in Tables 1 and 2). Similarly, surge estimates using the HSP approach for both the constant and time-varying $\lambda(t)$ cases are very similar, with differences in RMS errors of no more than 1.5% over the range of T_R = 50–1000 years for record lengths K = 50–10,000 years.

[43] However, for short record lengths, K = 25 years, 6% of the generated synthetic hurricane histories resulted in zero hurricane events over the record length. This indicates that in order to capture and represent decadal-scale climate variability, the record length must be long enough to capture the full decadal cycle, in this case variation in $\lambda(t)$ over 40 years.

5. Discussion

[44] To provide some perspective on our results, consider for example the surge-prone region of New Orleans, Louisiana. Prior to 2005, the historical surge record for the Louisiana coastline of the Gulf of Mexico included only a handful of severe surge events. At that time, Hurricane Camille (1969) was the most severe observed surge event for this region, with observed maximum surge on the open coast of 6.4 to 6.9 m. Following landfall of Hurricane Katrina in the vicinity of New Orleans in 2005, the historical surge population now reflected two large surge events, in which the observed maximum surge on the open coast for Hurricane Katrina was of the order of 20% higher than that of Hurricane Camille, 7.5 to 8.5 m [*IPET*, 2008]. Extreme-value surge estimates using the HSP approach for New Orleans prior to 2005 indicate that Hurricane Katrina's surge is associated with a return period larger than T_R = 1000 yr [*Resio et al.*, 2009]. Yet, reanalysis by the HSP approach when Hurricane Katrina is included reduces the return period of this surge event considerably. The question is then, How is the probability of these surges best characterized?

[45] To assess the specification of extreme surge probability, we consider two K = 100 year synthetic records (Table 5). In these records, between 9 and 15 landfall events

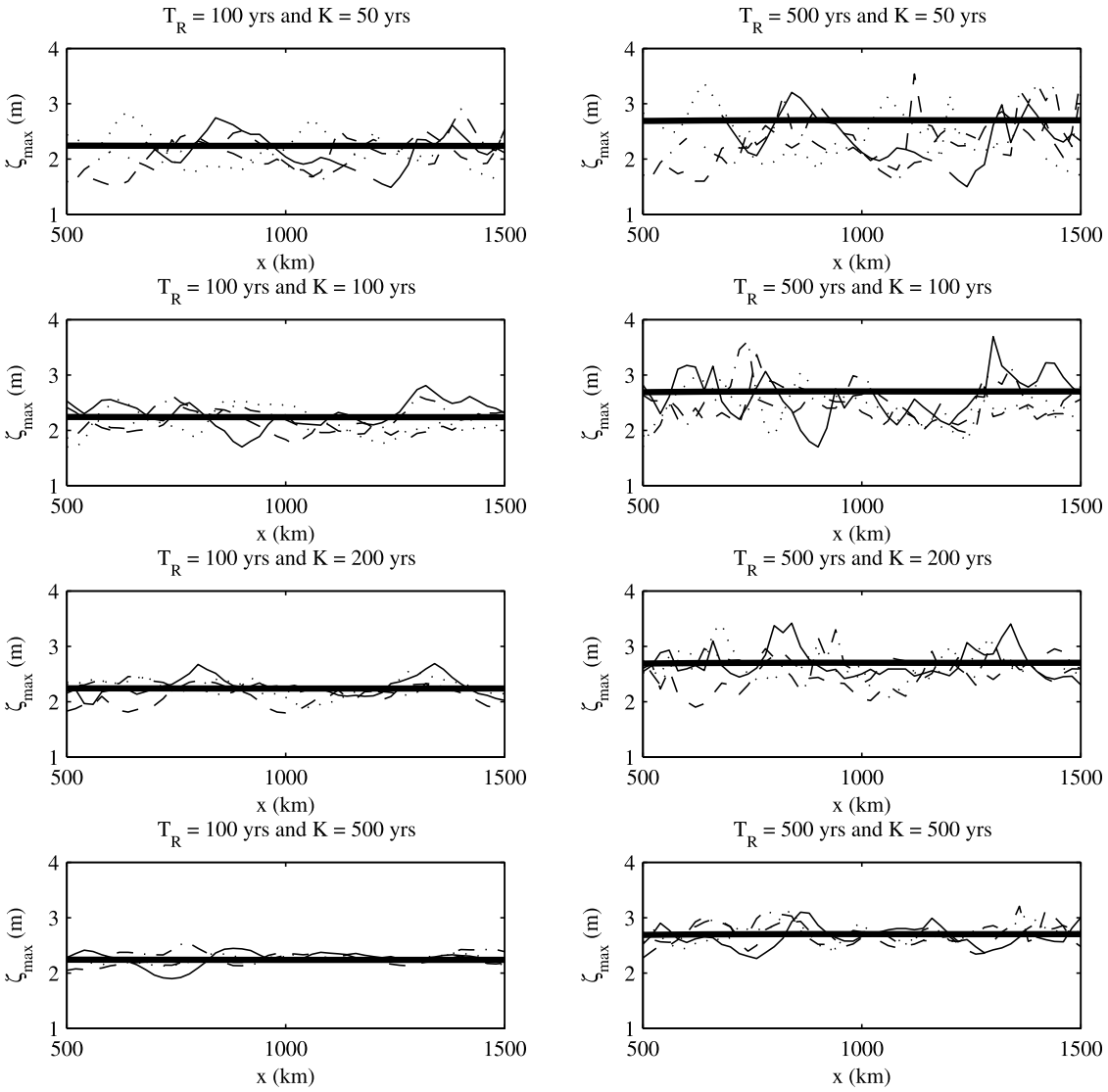

Figure 3. Alongshore variation in statistical surge estimates by historical surge population (HSP) approach as a function of varying record length (K) for the 1:1000 slope case. Solid line without symbols indicates assumed actual surge while each line with symbols represents the surge estimate for one synthetic history of length K.

resulted in surges greater than the peaks-over-threshold value. The highest surge in record A is 6% and 14% higher than the second highest surge, for the 1:1000 and 1:10,000 slope cases, respectively, while the highest surge in record B is 7% and 11% higher than the second- highest surge. In contrast, the largest central pressure deficit (Δp) in each record is only 3% larger than the second-largest Δp. In the following discussion, we assess the sensitivity of both the HSP approach and the JPM to removal of the most extreme event in the record.

[46] To assess HSP sensitivity to removal of a high surge, the surge stage frequency was estimated using the HSP approach by assuming that when K = 99 years, all but the highest surges are included in each record. This scenario is analogous to the New Orleans case when Hurricane Katrina is excluded. Similarly, to assess JPM sensitivity to removal of a large Δp, surge stage frequency was estimated using the JPM by assuming that when K = 99 years, all but the largest Δp are included in each record.

[47] Figure 5 shows that the HSP result is very sensitive to removal of a high surge from the record, whereas the JPM result is virtually unchanged when the largest Δp is removed. For example, the percentage of change in the 100-year return period surge by the HSP approach is between 6% and 27%. While this result is not surprising in view of the relative magnitude of the highest surge in the K = 100 year record, with respect to the next largest surge and the ranking and fitting method applied (section 2.1), it does indicate that application of the HSP approach is problematic. The estimated distributions by the HSP approach, in terms of both magnitude and shape, are very sensitive to incremental changes in sample size, as was also seen in the HSP results presented above. This is an artifact of a relatively short record length combined with the small spatial

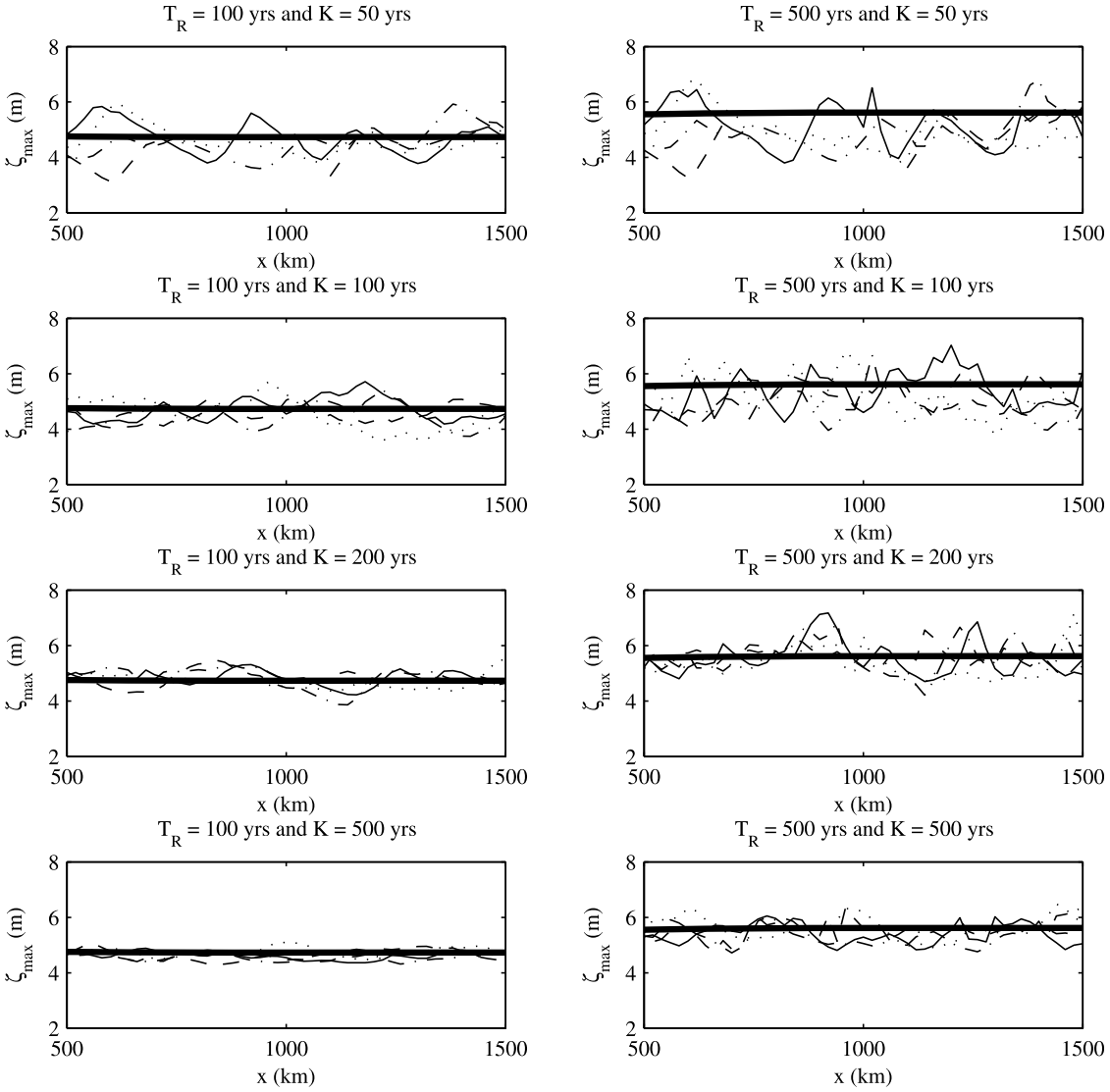

Figure 4. Alongshore variation in statistical surge estimates by historical surge population (HSP) approach as a function of varying record length (K) for the 1:10,000 slope case. Solid line without symbols indicates assumed actual surge while each line with symbols represents the surge estimate for one synthetic history of length K.

distance covered by extreme surges and random alongshore landfall positions.

[48] Given the small sample sizes for large surges, for example in the Gulf of Mexico, local extreme-value probabilities given by the HSP approach are heavily influenced by single surge events. In contrast, the surge extreme-value probabilities given by the JPM draw from contributions throughout the meteorological parameter space. Figure 6 shows the relevant parameter space contributing to selected return period estimates for the 1:10,000 slope case. Whereas one surge event, or individual (Δp, R_p, x_0) set, is used to prescribe T_R = 100 years in the HSP approach, in the JPM a whole range of (Δp, R_p, x_0) is used. For the T_R = 100 year surge, events making landfall as far away as 550 km from the point of interest contribute to this surge probability, and storm size and pressure deficit span from 8 to 120 km and from 70 to 130 mbars, respectively. Furthermore, the JPM result is not sensitive to changes in the hurricane parameter population, as seen in Figure 5. Thus, not only does the JPM approach more fully capture the relative importance of nonhistorical landfall positions and storm characteristics, the JPM approach also is not sensitive to small changes in the defining sample.

[49] Another way to consider the relative impact of sample size on extreme surge specification is to consider how often the HSP and JPM can be expected to yield a result close to the actual result, $\zeta_{JPM-actual}$ or $\bar{\zeta}_{HSP-100000}$. For the record lengths K = 50 and 100 years, cumulative distribution functions F of absolute errors in the 100-year return period surge, $|\Delta\zeta_{\max}(n)$, were developed (Figure 7). In the case of the HSP approach, only those records yielding a result were considered in developing the cumulative distribution function. Figure 7 shows that when analyzed with JPM, 90% of the records yield a T_R = 100 year surge that is within 7% of the actual result. In contrast, only 30% to 40% of the records analyzed with the HSP approach yield similar

Table 4. Alongshore Variation in Surge Estimates[a]

K (yr)	T_R = 50 Years	T_R = 100 Years	T_R = 500 Years	T_R = 1000 Years	Average Standard Deviation (m) [Percent of Mean Alongshore Surge Estimate]
			Alongshore Standard Deviation (m) for 1:1000 Slope Case		
50	0.27	0.30	0.39	0.43	0.35 [14%]
100	0.22	0.23	0.34	0.42	0.30 [12%]
200	0.16	0.16	0.27	0.36	0.23 [9%]
500	0.10	0.10	0.19	0.26	0.16 [6%]
1,000	0.07	0.07	0.14	0.19	0.11 [5%]
10,000	0.02	0.02	0.04	0.05	0.03 [1%]
100,000	0.01	0.01	0.01	0.02	0.01 [0%]
			Alongshore Standard Deviation (m) for 1:10000 Slope Case		
50	0.52	0.57	0.75	0.85	0.68 [13%]
100	0.40	0.42	0.65	0.81	0.57 [11%]
200	0.29	0.29	0.51	0.68	0.44 [8%]
500	0.19	0.19	0.37	0.50	0.30 [6%]
1,000	0.13	0.13	0.26	0.35	0.21 [4%]
10,000	0.04	0.04	0.08	0.10	0.07 [1%]
100,000	0.02	0.01	0.03	0.04	0.02 [0%]

[a]Standard deviation represents the standard deviation with respect to the mean alongshore value. Average standard deviation represents average for all T_R between 50 and 1000 years.

accuracy. This shows that, with respect to the HSP approach, the JPM provides a much more accurate and stable estimate of extreme surge probability.

[50] There are two spatial scales contributing to uncertainty in hurricane surge statistics: (1) inhomogeneity of the storm population and (2) inhomogeneity of the storm response. Here, we have addressed the impact of the second scale. As discussed in section 3, the uncertainty in the JPM method that is due to both scales is estimated to be 1.86 times the uncertainty that is due to inhomogeneity of the storm response. Considering the K = 25 year record, the total JPM RMS errors increase on average to 0.25 m and 0.45 m for the 1:1000 and 1:100,000 slope cases, respectively. These JPM RMS errors are still considerably smaller than the HSP RMS error, with the adjusted JPM RMS error being about 50% to 60% of the HSP RMS error. For larger record lengths, the adjusted JPM RMS error is 30% to 45% of the HSP RMS error.

6. Conclusions

[51] By considering a straight, idealized coast, we conclude that use of the JPM over the HSP approach is preferable for evaluating hurricane surge extreme-value statistics. Even for relatively short records (e.g., K = 25 or 50 year) of hurricane meteorology, the JPM used with surge response functions produces extreme-value surge estimates within about 5% of the assumed actual values with no bias. In contrast, the performance of the HSP approach is strongly linked to record length. For the range of record lengths typically available, K typically less than 100 years, surge estimates can be expected to deviate from actual values by at least 9% and up to about 20% for record lengths of $K \leq 100$ years.

[52] Reliance on the HSP approach for extreme-value surge estimation is also problematic when a particular location's historical record contains a limited number of surge events, despite the fact that the location is prone to hurricane activity. The idealized coast analysis presented above shows that the number of surge events over the specified threshold is often too low to yield meaningful statistics. For record lengths of $K \leq 50$ years, 10% to more than 60%, depending on K and the continental shelf slope, of the generated synthetic hurricane histories resulted in no statistical results from the HSP approach. When the lack of

Table 5. Sample Surge and Pressure Records When Record Length K = 100 Years[a]

Record A		Record B	
1:1000, 41, 9[b]	1:10000, 41, 10[b]	1:1000, 36, 12[b]	1:10000, 36, 15[b]
		Surge (m)	
2.32	5.17	2.48	5.53
2.18	4.52	2.32	4.96
2.17	4.26	2.24	4.40
2.04	4.17	2.20	4.29
1.89	4.12	1.91	4.22
1.87	3.57	1.78	4.19
1.39	2.82	1.67	4.16
1.16	2.71	1.64	3.83
0.99	2.28	1.55	3.64
	1.98	1.54	3.02
		1.53	2.99
		0.99	2.84
			2.57
			2.40
			2.02
		Central Pressure (mb)	
918		915	
921		918	
925		924	
927		930	
927		932	
929		933	
932		938	
933		940	
933		940	
935		940	
list truncated		list truncated	

[a]Only the 10 most intense central pressures are given. Most extreme surge and pressure are in bold.

[b]These three values are the slope, the number of landfalls on 2000-km coast, and the number of surge events ≥ peaks-over-threshold value, respectively.

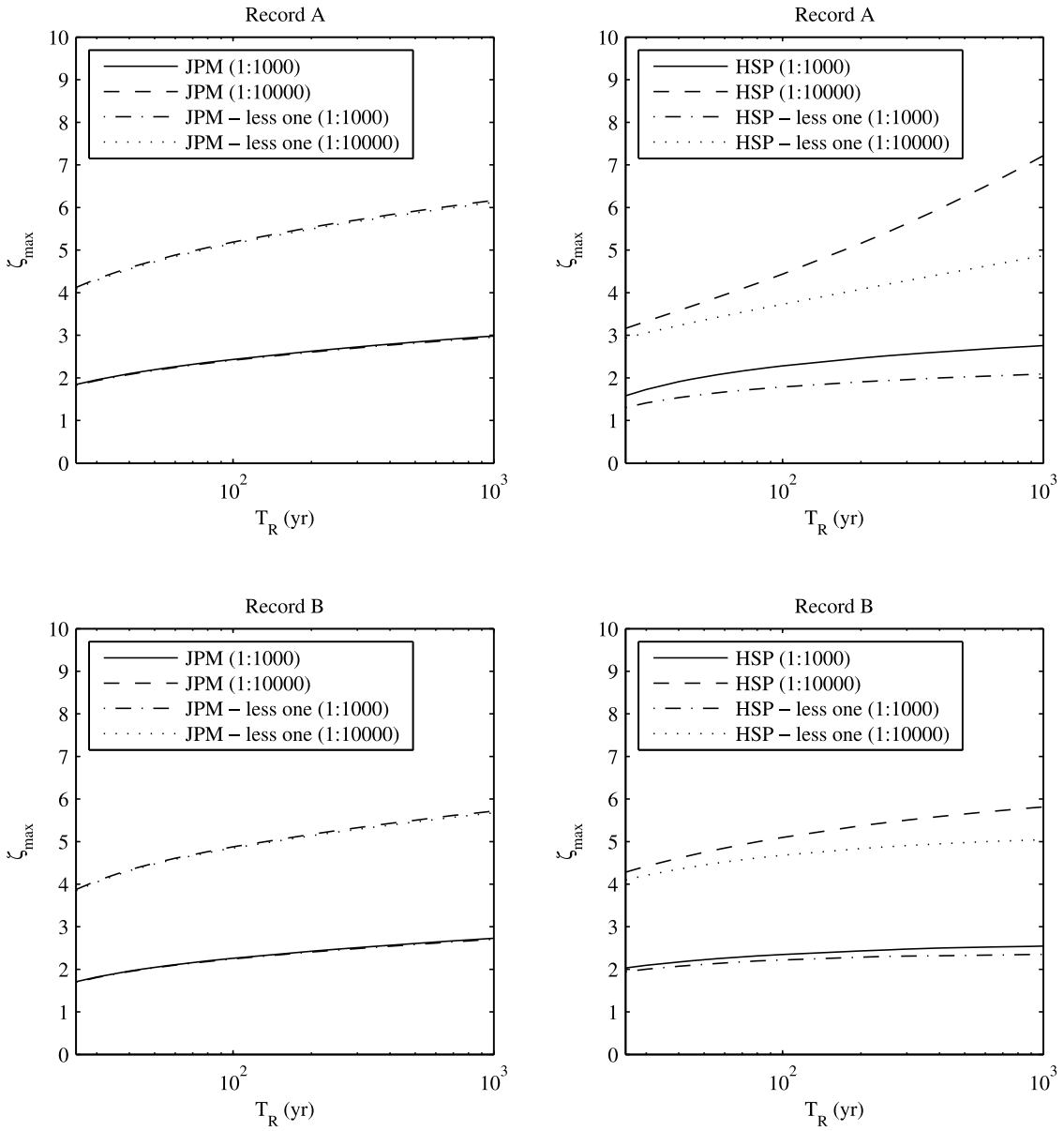

Figure 5. Surge stage frequency relationships for two synthetic records, A and B, developed using (left) the historical surge population (HSP) approach when the most extreme surge in the record is included and when it is excluded ("less one" in legend) and (right) the joint probability method (JPM) when the most extreme central pressure in the record is included and when it is excluded ("less one" in legend).

surge events in a given location's hurricane history is strictly due to the randomness inherent in hurricane landfall locations, surge estimates by the HSP approach will misleadingly underrepresent the surge risk. The JPM overcomes this limitation by considering the basin-wide hurricane population and by considering nonhistorical hurricane possibilities.

[53] Further emphasizing this disadvantage of the HSP approach is the alongshore variability in the probabilistic surge estimate from location to location. The idealized coast results presented above show that for short record lengths of $K = 50$ years, the standard deviation in surge is as much as 15% from location to location, with respect to the average alongshore surge estimate by the HSP approach. The implications of using the HSP approach are to artificially overestimate surge probabilities at some locations while artificially underestimating surge probabilities at other locations up-coast and down-coast. An underestimation (overestimation) of surge probability will lead to an underestimation (overestimation) of flood risk and ultimately will lead to an underdesign (overdesign) of coastal protection and infrastructures. Again, the JPM overcomes this shortcoming in the HSP approach by considering all hurricane possibilities at all locations along the coast to yield identical surge estimates at all coastal locations.

[54] Finally, the results above indicate that both the JPM and the HSP approach are robust in their ability to treat

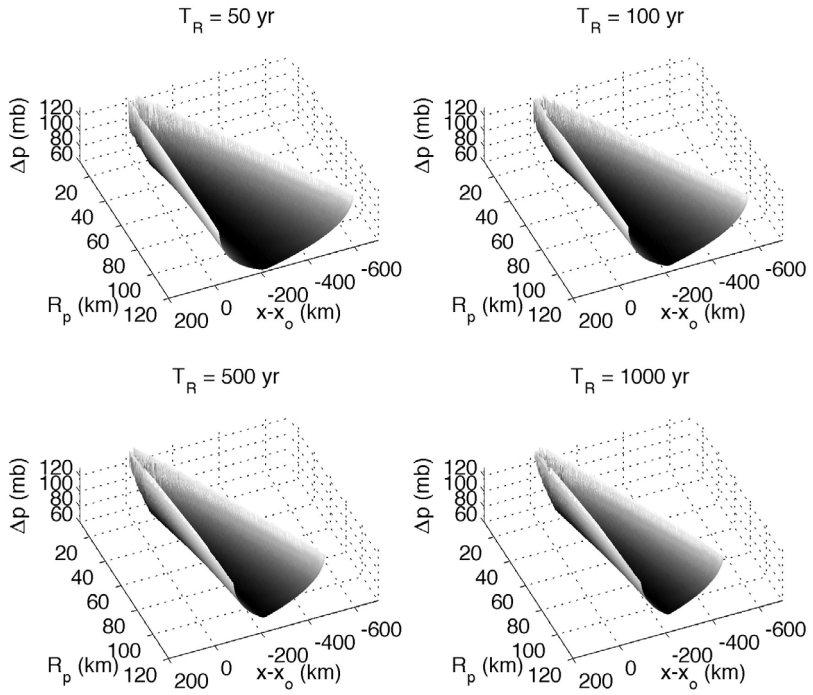

Figure 6. Surfaces of constant surge (constant return period) applied in the joint probability method (JPM) for the 1:10,000 case.

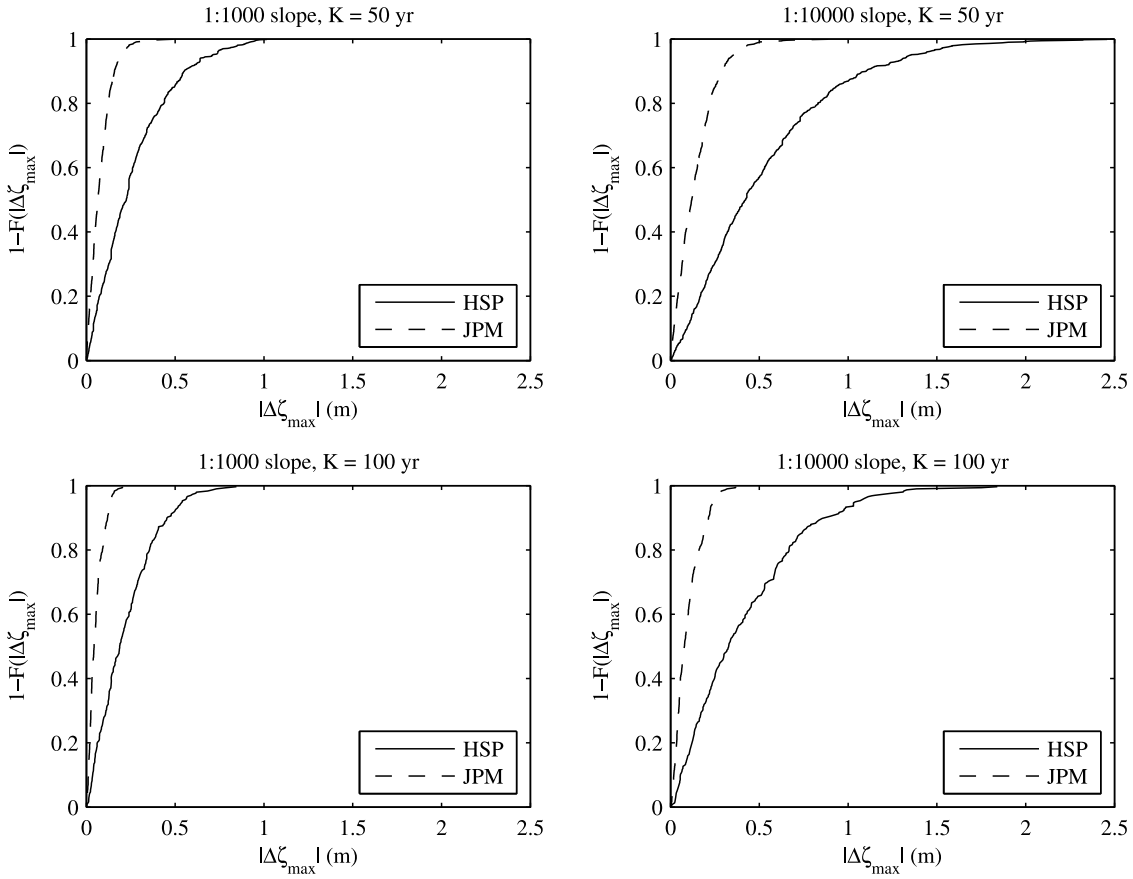

Figure 7. Cumulative distribution functions for absolute error in 100 year return period surge estimate when record length (top) K = 50 years and (bottom) 100 years.

decadal-scale climate variability so long as the record length contains the full decadal cycle. For the case of hurricane rates of occurrence in the Gulf of Mexico, a record length (K) greater than the cycle length of 40 years is required.

[55] In conclusion, with respect to the HSP approach, it has been demonstrated that the JPM is a more stable and accurate method for determining hurricane surge extreme-value statistics. In practical application of the JPM, the computational burden imposed by considering all hurricane possibilities is overcome by use of parameterized surge response functions. Relying on JPM-based probabilistic surge estimates will allow for more effective communication to the public about flood hazards as well as lead to more appropriate coastal planning, engineering design, and evacuation planning.

Notation

a an empirical constant.
a_i Gumbel coefficients.
b an empirical constant.
c an empirical constant.
c_p hurricane central pressure near landfall.
m rank for cumulative distribution.
$m(x)$ location-dependent constant.
p probability density function.
v_f hurricane forward speed near landfall.
x geographic location of interest.
x' dimensionless alongshore distance from location of interest to peak surge.
x_0 landfall location.
F cumulative distribution function.
GEV generalized extreme value.
HSP historical surge population (approach).
JPM joint probability method.
POT peaks over threshold.
K record length.
M storm surge rank.
N total number of surge records in the historical population.
P_{Ex} probability of exceedance.
P_{Non} probability of nonexceedance.
R_p hurricane pressure radius near landfall.
SRF surge response function.
T_R return period.
γ specific weight of water.
δ average distance between landfall location and peak alongshore surge normalized by R_p.
ε uncertainty in surge response.
σ normal distribution standard deviations.
$\zeta_{HSP\text{-}100,000}$ extreme-value surges by HSP approach when record length K = 100,000 years.
ζ_{HSP-K} extreme-value surges by HSP approach for record length K.
$\zeta_{JPM\text{-}actual}$ extreme-value surges by JPM when sampling distribution used.
ζ_{JPM-K} extreme-value surges by JPM for record length K.
$\Delta\zeta_{max}$ extreme-value surge error.
ζ_{max} hurricane surge response.
$\zeta'_{max}(x)$ dimensionless hurricane surge response at location of interest x.
θ hurricane track angle with respect to the shoreline.
λ constant hurricane rate of occurrence.
$\lambda(t)$ time-varying hurricane rate of occurrence.
ϕ continuous surge response function.
Δp central pressure deficit (peripheral pressure minus c_p).
Δt time interval of interest.
Δx coastal section length of interest.
Λ_I probability density of individual parameter i.
overbars normal distribution mean values.

[56] **Acknowledgments.** This research was supported by the U.S. Army Engineer Research and Development Center, Coastal and Hydraulics Laboratory, and the Office of Science (BER), U.S. Department of Energy (grant DE-FG02-08ER64644). The use of trade names does not constitute an endorsement in the use of these products by the U.S. Government. Finally, the authors wish to thank the journal reviewers for their insightful comments, ultimately leading to a more comprehensive and clear presentation of this research.

References

Agbley, S. K., and D. R. Basco (2008), An evaluation of storm surge frequency-of-occurrence estimator, paper presented at Solutions to Coastal Disasters Conference, Am. Soc. of Civ. Eng., Oahu, Hawaii.

Borgman, L. E., et al. (1992), Empirical simulation of future hurricane storm histories as a tool in engineering and economic analysis, paper presented at the Fifth International Conference on Civil Engineering in the Ocean, Am. Soc. of Civ. Eng., College Station, Tex.

Bunya, S., et al. (2010), A high-resolution coupled riverine flow, tide, wind, wind wave, and storm surge model for Southern Louisiana and Mississippi. Part I: Model development and validation, *Mon. Weather Rev.*, *138*(2), 345–377, doi:10.1175/2009MWR2906.1.

Chouinard, L. E., C. Liu, and C. K. Cooper (1997), Model for the severity of hurricanes in the Gulf of Mexico, *J. Waterw. Port Coastal Ocean Eng.*, *123*(3), 120–129, doi:10.1061/(ASCE)0733-950X(1997)123:3(120).

Dietrich, J. C., et al. (2010), A high-resolution coupled riverine flow, tide, wind, wind wave, and storm surge model for Southern Louisiana and Mississippi. Part II: Synoptic description and analysis of Hurricanes Katrina and Rita, *Mon. Weather Rev.*, *138*(2), 378–404, doi:10.1175/2009MWR2907.1.

Ho, F. P., and V. A. Myers (1975), Joint probability method of tidal frequency analysis applied to Apalachicola Bay and St. George Sound, Florida, U.S. Dep. of Commer., Washington, D. C.

Holland, G. J. (1980), Tropical cyclone structure in the southwest Pacific, *Bull. Am. Meteorol. Soc.*, *61*(9), 1132.

Interagency Performance Evaluation Task Force (IPET) (2008), Performance evaluation of the New Orleans and Southeast Louisiana Hurricane Protection System, in *Engineering and Operational Risk and Reliability Analysis*, vol. 8, report, U.S. Army Corps of Eng., Washington, D. C.

Irish, J. L., and D. T. Resio (2010), A hydrodynamics-based surge scale for hurricanes, *Ocean Eng.*, *37*(11–12), 1085–1088, doi:10.1016/j.oceaneng.2010.04.002.

Irish, J. L., D. T. Resio, and J. J. Ratcliff (2008), The influence of storm size on hurricane surge, *J. Phys. Oceanogr.*, *38*(9), 2003–2013, doi:10.1175/2008JPO3727.1.

Irish, J. L., D. T. Resio, and M. A. Cialone (2009), A surge response function approach to coastal hazard assessment. Part 2: Quantification of spatial attributes of response functions, *Nat. Hazards*, *51*(1), 183–205, doi:10.1007/s11069-009-9381-4.

Levinson, D. H., P. J. Vickery, and D. T. Resio (2010), A review of the climatological characteristics of landfalling Gulf hurricanes for wind, wave, and surge hazard estimation, *Ocean Eng.*, *37*(1), 13–25, doi:10.1016/j.oceaneng.2009.07.014.

Myers, V. A. (1975), Storm Tide Frequencies on the South Carolina Coast, U.S. Dep. of Commer., Washington, D. C.

Peterson, T. C., and M. O. Baringer (2009), State of the climate in 2008, *Bull. Am. Meteorol. Soc.*, *90*, S1–S196, doi:10.1175/BAMS-90-8-StateoftheClimate.

Resio, D. T., J. Irish, and M. Cialone (2009), A surge response function approach to coastal hazard assessment. Part 1: Basic concepts, *Nat. Hazards*, *51*(1), 163–182, doi:10.1007/s11069-009-9379-y.

Scheffner, N. W., et al. (1996), Empirical simulation technique based storm surge frequency analysis, *J. Waterw. Port Coast. ASCE*, *122*(2), 93–101.

Thompson, E. F., and V. J. Cardone (1996), Practical modeling of hurricane surface wind fields, *J. Waterw. Port Coastal Ocean Eng.*, *122*(4), 195–205, doi:10.1061/(ASCE)0733-950X(1996)122:4(195).

Tonkin, H., G. J. Holland, N. Holbrook, and A. Henderson-Sellers (2000), An evaluation of thermodynamic estimates of climatological maximum potential tropical cyclone intensity, *Mon. Weather Rev.*, *128*, 746–762, doi:10.1175/1520-0493(2000)128<0746:AEOTEO>2.0.CO;2.

D. Divoky, AECOM, 1360 Peachtree St. NE, Ste. 500, Atlanta, GA 30309, USA.

J. L. Irish, Department of Civil and Environmental Engineering, Virginia Polytechnic Institute and State University, Postal Code 0105, Blacksburg, VA 24061, USA. (jirish@vt.edu)

D. T. Resio, College of Computing, Engineering and Construction, University of North Florida, Jacksonville, FL 32224, USA.